

RESEARCH

Open Access



Structural Performance of RC and R-ECC Dapped-End Beams Based on the Role of Hanger or Diagonal Reinforcements Combined by ECC

Bashar S. Mohammed^{1*} , Muhammad Aswin^{1,2}, M. S. Liew¹ and Noor Amila Wan Abdullah Zawawi¹

Abstract

Twenty-seven large-scale beams with dapped-end have been prepared, cast and tested to failure in the three points loading arrangement. One control beam has been designed in accordance with requirement of standard code while the dapped-end reinforcement scheme of other beams has been derived from the control beam. In selected beams, engineered cementitious composites (ECC) has been utilized in the dapped-end region. The test results exhibited that DR is more appropriate and higher capacity than HR in resisting the shear force. In addition, the reinforced engineered cementitious composites dapped-end beams (R-ECC-DEB) showed higher structural performance compared to the normal reinforced concrete dapped-end beams (RC-DEBs). The strength of ECC also has direct effect on the failure capacity of the R-ECC-DEB, in which higher strength of ECC leads to higher failure capacity of R-ECC-DEB.

Keywords: dapped-end beam, hanger reinforcement, diagonal reinforcement, ECC, failure load, final deflection, crack pattern, failure mode

1 Introduction

Precast reinforced concrete dapped-end beams (RC-DEBs) are widely being used in multi-story car park (Fu 2004; Herzinger 2008; Forsyth 2013; Botros et al. 2017), the reinforced concrete (RC) buildings (Forsyth 2013; Botros et al. 2017; Ahmad et al. 2013), long-span and pedestrian bridges (Mohammed and Mahmoud 2015; Herzinger and Elbadry 2007), and concrete bridge girders (Taher 2005). The nibs of precast RC-DEBs are frequently supported by columns, beam-to-beam connections, inverted T-beams (ledger beams), cantilevers or corbels. Due to the notching or recessing at the ends, RC-DEBs have more lateral stability at the supports than normal

precast RC beams. In addition, RC-DEBs allow reduction in the total height of constructions.

Several studies have been carried out to investigate the capacity of RC-DEBs. Wang et al. (2005) have studied the shear strength of dapped-end beam (DEB) and suggested that the height of nib should be larger than 0.45 times the height of beam. Peng (2009) has utilized proper anchorage and adequate hanger reinforcements to achieve good ductility and higher shear strength of RC-DEBs. Mattock (2012) has concluded that variation of nominal shear span and nib height can lead to different shear strength capacity of RC-DEBs. Nagrodzka-Godycka and Piotrkowski (2012) have carried out an experimental investigation of RC-DEBs subjected to the vertical and the inclined forces at the supports. They have reported that dapped-end beams which loaded by only the vertical forces exhibit higher load carrying capacity compared to the dapped-end beams that subjected to the inclined forces.

Mattock and Theryo (1986) have experimentally investigated five precast-prestressed concrete T-beams with

*Correspondence: bashar.mohammed@utp.edu.my

¹ Department of Civil and Environmental Engineering, Universiti Teknologi PETRONAS, 32610 Bandar Seri Iskandar, Perak Darul Ridzuan, Malaysia

Full list of author information is available at the end of the article
Journal information: ISSN 1976-0485 / eISSN 2234-1315

different dapped-end reinforcement schemes. They indicated that by draping a half or more the pre-stressing strands/tendons through the nib has led to significantly increasing the load failure of RC-DEBs. Lu et al. (2003) have shown that the shear strength of DEBs increases with increasing the concrete compressive strength and number of nib flexural reinforcements. While reducing of the nominal shear span-depth ratio leads to increase the shear strength of RC-DEBs. Taher (2005) has reported that strengthening of dapped-end region can lead to increase the shear strength of RC-DEBs. Herzinger (2008) has proved that use of single and double head stud reinforcements in dapped-end region will improve the performance of these beams in comparison to the conventional reinforcements. This method can reduce congestion of dapped-end reinforcements. Mohamed and Elliott (2008) have studied RC-DEBs made of steel fiber self-compacting concrete (SF-SCC). They have reported that better shear strength of those beams leading to reduce the amount of dapped-end reinforcements. Huang and Nanni (2006) as well as Nagy-György et al. (2012) have proved that CFRP strengthening at dapped-end region resulting in higher shear strength capacity of RC-DEBs.

Aswin et al. (2015a) have analyzed the tests data of 111 RC-DEBs available in the literatures, and concluded that the shear failure is the dominating failure mode of these beams. Dapped-end beams are usually subjected to the high stress flows due to the geometry discontinuity at the end of beams, known as D-region (Ahmad et al. 2013; Herzinger and Elbadry 2007; Mohamed and Elliott 2008; Huang and Nanni 2006; Aswin et al. 2015b). Strain distribution at D-regions is significantly non-linear (Schlaich and Schafer 1991), then the first crack is always initiated from the re-entrant corner of the RC-DEBs (Forsyth 2013; Wang et al. 2005; Aswin et al. 2015b; Mattock and Chan 1979; Moreno-Martínez and Meli 2014). Therefore, researchers have suggested to providing the suitable reinforcements close to re-entrant corner to resist the diagonal cracks that may occurs in dapped-end region (Huang and Nanni 2006; Mattock and Chan 1979; Huang 2000).

To anticipate the diagonal cracks emanating from re-entrant corner, in general, vertical stirrups as hanger reinforcement (HR) has been utilized. However, Wang et al. (2005) have reported that inclined stirrups and longitudinal bent reinforcements have more influence on the shear strength than vertical stirrups. Forsyth (2013) has reported that the inclined HR significantly reduces the crack width and crack propagation rate compared to the vertical HR. The inclined hanger reinforcements can delay the onset of cracking and increase the strength capacity by nearly 30% as compared to similar specimens with the vertical HR. Desnerck et al. (2016) have

reported that the beams with less nib reinforcements exhibit lower load carrying capacity than beams with complete nib reinforcements, while inadequate diagonal reinforcements lead to the lowest load carrying capacity by approximately 40%.

Several attempts to improve the capacity of dapped-end beams have been carried out including the use of precast-prestressed concrete, high strength concrete, various different strengthening techniques, head stud reinforcement, steel fiber-self compacting concrete, CFRP strengthening, inclined stirrup and longitudinal bent reinforcement, etc. Aswin et al. (2015b) have utilized the engineered cementitious composite (ECC) in dapped-end region, and reported that occur improvement in the failure load and deflection capacity of RC-DEBs.

It has been proved that ECC has unique features of tensile ductility and intrinsic crack width controlling capacity using less than 2% volume fraction of polyvinyl alcohol (PVA) fiber. ECC also has wide range of strain capacity up to 8% (Li 1993, 2008; Fukuyama et al. 2000). This characteristic is attributed to the fiber ability in the crack bridging (Lepech and Li 2008).

The main aim of the research work reported in this paper is to investigate the role of hanger reinforcement (HR) or diagonal reinforcement (DR), as well effect of use of ECC on the structural performance of DEBs. Structural performance involves failure load, final deflection capacity, pre-peak and post-peak response, crack pattern and failure mode.

2 Experimental Program

2.1 Design of Steel Reinforcement for Dapped-End Region

One control beam has been designed in accordance with the requirements of PCI code (P. D. Handbook 2010). Five potential failure modes of RC-DEB have been specified as shown in Fig. 1. These failure modes are: (1) flexure and axial tension in extended end, (2) direct vertical shear between nib and un-dapped portion, (3) diagonal tension initiating from re-entrant corner, (4) diagonal tension in the nib area, and (5) diagonal tension in un-dapped portion.

2.2 Preparations of Beams

Twenty-seven large-scale beams with dapped-end have been prepared, cast, cured and tested up to failure at age of 28 days. These beams have dimensions of 1800 mm overall length, 110 mm length of nib portion, 140 mm height, and 120 mm width. The un-dapped portion dimensions are 120 mm width and 250 mm height.

Based on the reinforcement configuration of DEB-3 as the control beam, the dapped-end reinforcements are varied and developed to provide the requirement of dapped-end reinforcements of other beams. All

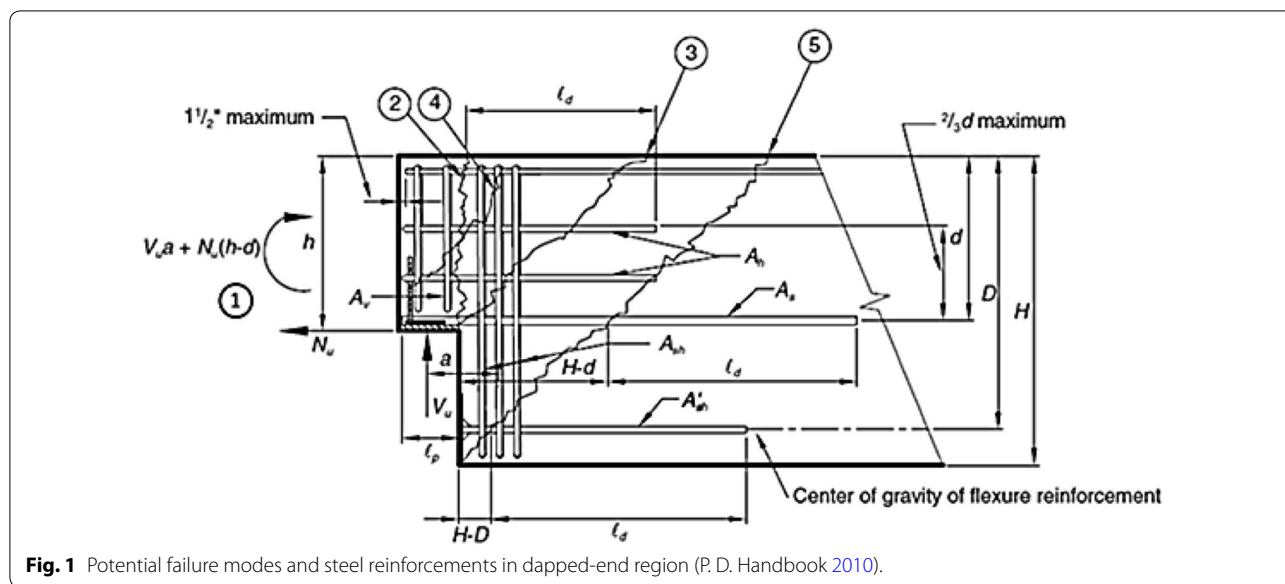


Fig. 1 Potential failure modes and steel reinforcements in dapped-end region (P. D. Handbook 2010).

investigated beams in this study consist of two groups. The first group includes 15 DEB specimens which involves different HR scheme and combined by using ECC. The second group contains of 12 DEB specimens with different DR configuration that combined by utilizing HR and ECC. The ECC placement and the steel reinforcement configuration of all DEB specimens can be seen in Figs. 2 and 3, while the steel reinforcement details are presented in Table 1.

To provide the concrete confinement strength sufficiently, closed stirrup with two legs were assembled for nib vertical reinforcement (NVR), HR and shear link/stirrup (St). To reduce the reinforcement congestion in dapped-end region and to provide adequate anchorage of longitudinal reinforcements, the 90° bend for anchorage has been replaced by using the cross steel bars which welded at their ends, such as the top bars, nib flexure reinforcement (NFR) and beam main flexure reinforcement (BMFR), conforming to the requirements of ACI code (A. Committee and I. O. f. Standardization 2008) and also as suggested by Mattock and Chan (1979).

For DR, the idea is similar to HR but placed incline approximately at 45° with beam axis. The cross steel bars were also welded at both ends either at top and bottom of DR. Especially for nib horizontal reinforcement (NHR), the U-bar is better to be used in providing adequate anchorage and easy installation. The tensile tests of related steel bars have been conducted. According to the tensile test of two samples per each bar diameter, the average yield stress of steel bars of 8 mm and 10 mm diameter are obtained as 386.74 MPa, and 470.23 MPa, respectively.

2.3 Mix Proportions, Samples Preparation and Experimental Setup

NSC has been used for RC-DEBs along the beam, while R-ECC-DEBs utilize ECC-1 or ECC-2 that only placed in the dapped-end region. For ECC-2, fly ash (FA) content is lower than ECC-1, in which the cement-FA ratio is 0.6. The utilizing of silica fume (SF) of 10% of the total weight of cement and fly ash is intended to improve the micro-filling effect on the ECC matrix and improve the composites matrix strength. Further, to anticipate the domination of fibers rupture than their pull-out, need to treat the fibers surface by oiling (with the oiled fiber volume fraction of 0.6%), so higher elongation or strain of composites will be achieved. The mix proportions of NSC and ECC are shown in Table 2. Type I Ordinary Portland Cement, water, the washed Perak river sand with approximate particle size of 0.3–1.2 mm and the crushed limestone with maximum particle size of 10 mm have been used in NSC substrate. For ECC, super plasticizer with type of Polycarboxylate Ether (PCE), as well PVA fibers of 18 mm length have been used.

To ensure flow ability, passing ability and filling ability of ECC under its own weight in narrow area at the congested steel reinforcement in the dapped-end region, self-compacting ECC (SC-ECC) has been developed. This is important to minimize segregation and bleeding of fresh ECC, as well as to ensure the honeycomb free of hardened ECC and to get the optimum bonding strength between ECC and steel bars. To assess the fresh properties of SC-ECC, four tests have been undertaken which cover: slump flow, T_{500} -slump flow, V-funnel and L-box. Test results are shown in Table 3, which exhibits that the ECC mixture has fresh

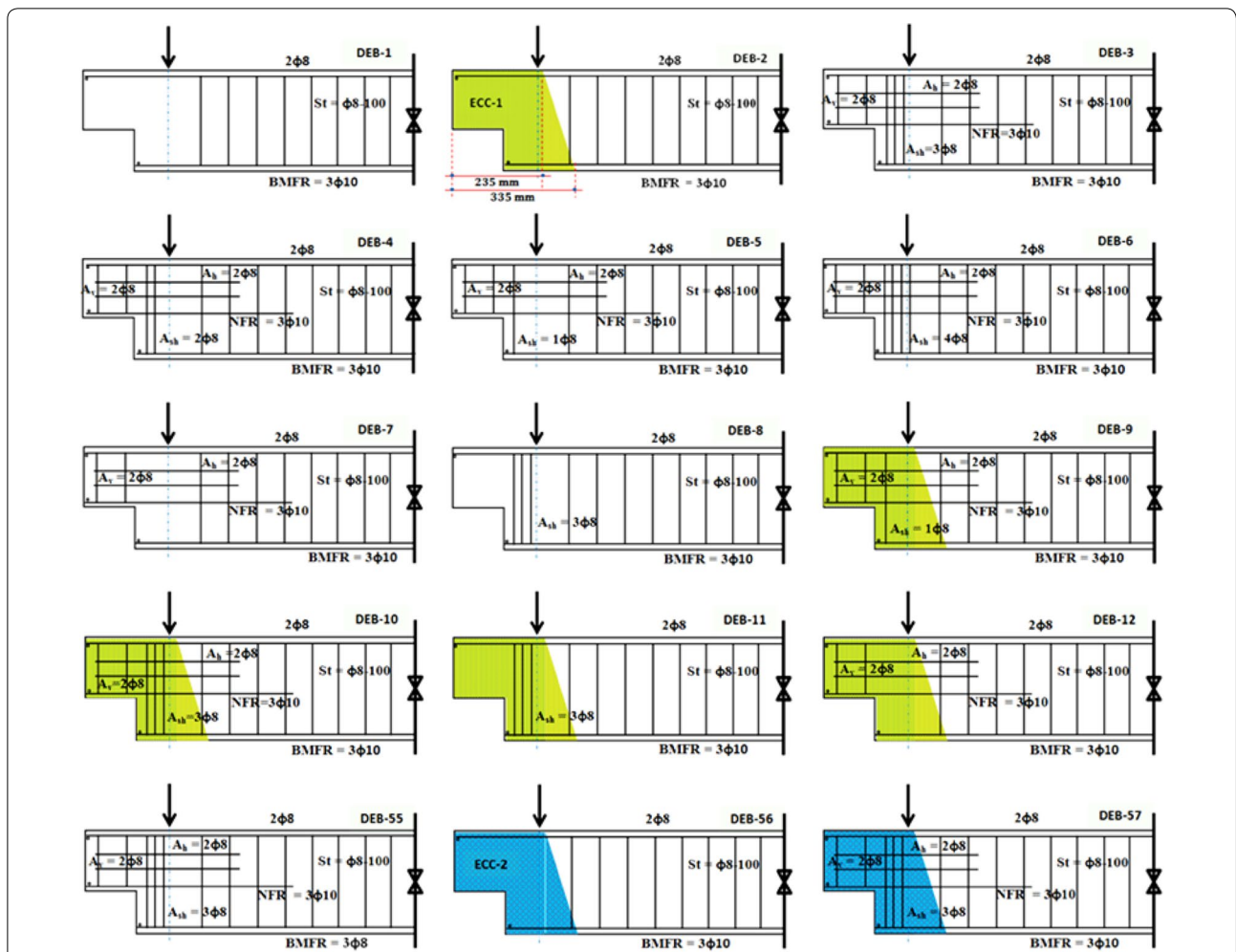


Fig. 2 The steel reinforcement configuration of DEBs in the first group.

properties satisfying the self-compacting requirements conforming to EFNARC (S.-C. C. E. P. Group 2005).

NSC and ECC samples have been prepared, casted and tested. Different samples have been created in accordance with the test requirement, such the compressive test, splitting tensile test, elastic modulus test, Poisson ratio test, flexural test, direct tensile test, density of the hardened concrete/ECC test, and permeability test. The test procedure follows the related testing methods. The test results of mechanical properties of the hardened NSC and ECC are shown in Table 4.

The typical experimental setup for the DEBs testing was shown in Fig. 4. To measure the vertical deflection of beams, Linear Variable Differential Transducer (LVDT) has been located at soffit of DEB specimen. All beams are subjected to the three point loading up to failure with loading rate of 0.15 kN/s. No axial tension force was applied.

3 Results and Discussion

3.1 Stress–Strain Relationship of NSC and ECC Samples

The stress–strain relationships for NSC/ECC was shown in Fig. 5a, b for compression and direct tensile, respectively. NSC shows a marginal descending branch after the peak stress is achieved. Due to its brittleness, the sudden failure is occurred when the peak stress is reached, while ECC shows plastic deformation characterized by the descending part of the curve due to its ductile behavior.

Meantime, the direct tensile test is used to measure ability of NSC/ECC to resist tensile force or cracks. ECC has larger tensile strength and strain capacity than NSC. Due to its brittleness, NSC fails suddenly after peak-stress is reached. Unlike NSC, ECC can develop pseudo-strain hardening after first crack, and at post-peak stage, ECC still has ability to perform larger plastic deformation up to failure, which characterized by tension softening. This is due to proper tailoring between fibers,

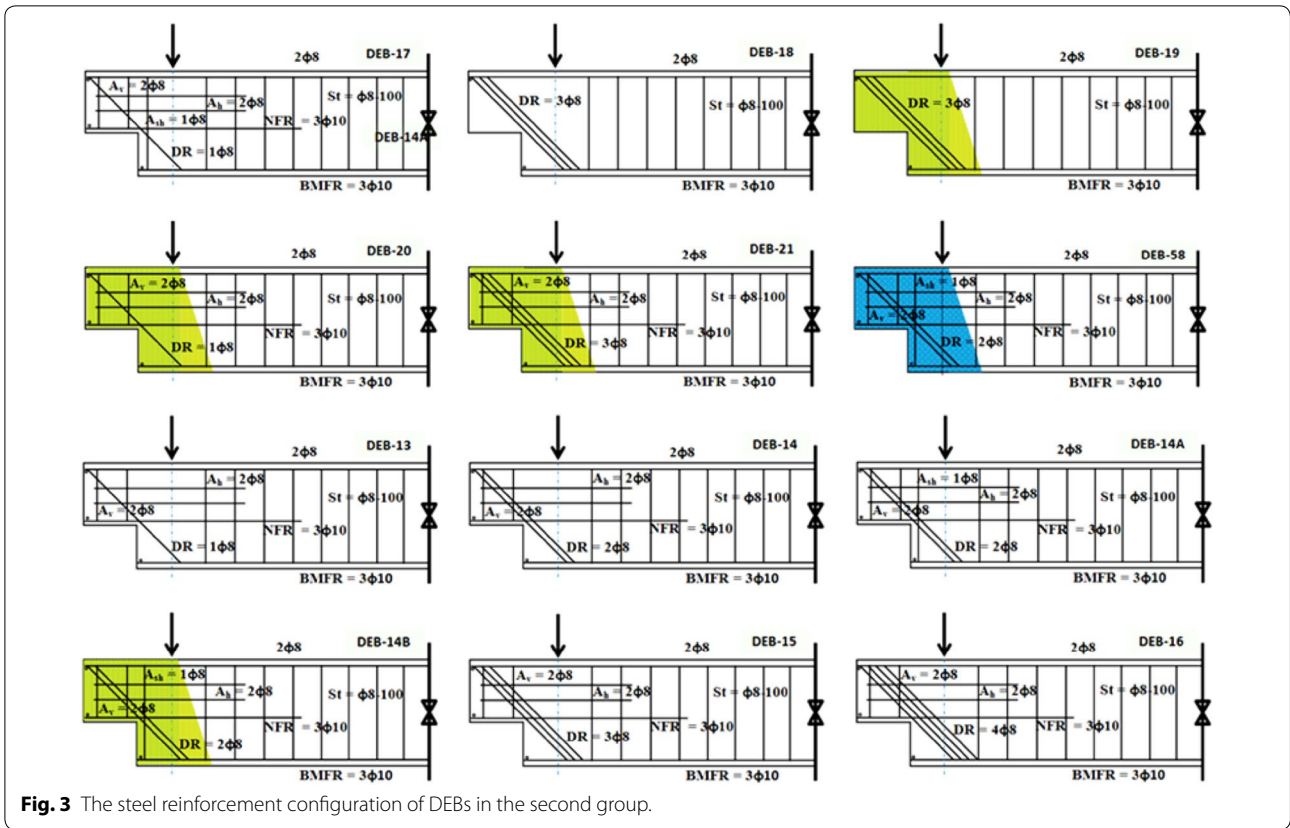


Fig. 3 The steel reinforcement configuration of DEBs in the second group.

matrix and fiber/matrix interface; ECC can develop fiber crack bridging behavior. Moreover, ECC-2 fails with the largest plastic deformation in which the tensile strain capacity reaches over 4%. By oiling treatment of the PVA fibers surface, the oiling can decrease the chemical bond strength, interfacial friction and surface abrasion of PVA fibers. The sliding between fibers and the composites matrix will achieve and improve the elongation or tensile strain capacity of ECC-2.

3.2 Load–Deflection Relationship of NSC and ECC Samples

Figure 6 shows the load–deflection curve of the NSC/ECC obtained from flexural test. NSC is subjected to sudden rupture after reach its peak stress, while ECC develops fiber crack bridging behavior. ECC shows flexural ability up to large number of plastic deformation even at wider cracks, therefore ECC failure is gradual.

3.3 The Failure Load and Final Deflection Capacity for the Beams in the First Group

The test results of the DEB specimens in the first group are given in Fig. 7. They have exhibited that the variations made to this parameter (related to the HR) provided the changes of the failure load and final deflection capacity of the DEB specimens.

The DEB-1 was a reference beam casted using the NSC along the beam and without any dapped-end reinforcements. As a result, the DEB-1 had the lowest capacity in the failure load and deflection. Referring to the ACI code (2008) and the PCI code (2010), the ultimate shear strength capacity of concrete (V_{uc}) can be determined by using Eq. 1.

$$V_{uc} = \varphi \left(2\lambda bd \sqrt{f'_c} \right) \tag{1}$$

where $\varphi = 0.75$ is the strength reduction factor and $\lambda = 1$ is the concrete coefficient for the NSC. Based on this formula, it can be obtained that $V_{uc} = 10.90$ kN. The failure load (P_{uc}) that was resisted by the DEB-1 was 12.05 kN. This value was quite close to the experimental result, where the analysis-test result ratio was 0.9577.

By comparing the DEB-1 and the DEB-3 specimen, it was clear that the dapped-end reinforcements improved the capacity of the DEB. The DEB-3 reached the failure load of 105.26 kN and final deflection capacity of 29.63 mm whilst the DEB-1 only achieved the failure load of 12.58 kN and final deflection capacity of 5.43 mm. In this case, the use of the dapped-end reinforcement in the DEB-3 provided a significant capacity increment of the failure load of 736.72% and final deflection capacity of

Table 1 The steel reinforcement details of DEBs.

No.	Spec. No.	Compressive strength		Splitting tensile strength		Direct tensile strength		NHR	NVR	HR	DR	Stirrup	Yield stress	NFR	BMFR	Yield stress	Top rebar	Yield stress
		NSC	ECC	NSC	ECC	NSC	ECC											
		f'_c MPa	f'_{cE} MPa	f_{stc} MPa	f_{stE} MPa	f_{tc} MPa	f_{tE} MPa											
1	DEB-1	27.10	-	2.53	-	1.36	-	-	-	-	-	φ8-100	387	-	3φ10	470	2φ8	387
2	DEB-2	27.10	84.00	2.53	6.42	1.36	4.87	-	-	-	-	φ8-100	387	-	3φ10	470	2φ8	387
3	DEB-3	27.00	-	2.52	-	1.34	-	2φ8	2φ8	3φ8	-	φ8-100	387	3φ10	3φ10	470	2φ8	387
4	DEB-4	27.10	-	2.53	-	1.36	-	2φ8	2φ8	2φ8	-	φ8-100	387	3φ10	3φ10	470	2φ8	387
5	DEB-5	27.80	-	2.56	-	1.40	-	2φ8	2φ8	1φ8	-	φ8-100	387	3φ10	3φ10	470	2φ8	387
6	DEB-6	27.80	-	2.56	-	1.40	-	2φ8	2φ8	4φ8	-	φ8-100	387	3φ10	3φ10	470	2φ8	387
7	DEB-7	27.80	-	2.56	-	1.40	-	2φ8	2φ8	-	-	φ8-100	387	3φ10	3φ10	470	2φ8	387
8	DEB-8	27.60	-	2.56	-	1.38	-	-	-	3φ8	-	φ8-100	387	-	3φ10	470	2φ8	387
9	DEB-9	27.60	84.00	2.56	6.42	1.38	4.87	2φ8	2φ8	1φ8	-	φ8-100	387	3φ10	3φ10	470	2φ8	387
10	DEB-10	27.60	84.00	2.56	6.42	1.38	4.87	2φ8	2φ8	3φ8	-	φ8-100	387	3φ10	3φ10	470	2φ8	387
11	DEB-11	27.60	82.50	2.56	6.29	1.38	4.77	-	-	3φ8	-	φ8-100	387	-	3φ10	470	2φ8	387
12	DEB-12	27.80	82.50	2.56	6.29	1.40	4.77	2φ8	2φ8	-	-	φ8-100	387	-	3φ10	470	2φ8	387
13	DEB-55	27.00	-	2.52	-	1.34	-	2φ8	2φ8	3φ8	-	φ8-100	387	3φ10	3φ8	470; 387	2φ8	387
14	DEB-13	27.80	-	2.58	-	1.37	-	2φ8	2φ8	-	1φ8	φ8-100	387	3φ10	3φ10	470	2φ8	387
15	DEB-14	27.80	-	2.58	-	1.37	-	2φ8	2φ8	-	2φ8	φ8-100	387	3φ10	3φ10	470	2φ8	387
16	DEB-14A	28.10	-	2.62	-	1.41	-	2φ8	2φ8	1φ8	2φ8	φ8-100	387	3φ10	3φ10	470	2φ8	387
17	DEB-14B	28.10	83.20	2.62	6.37	1.41	4.86	2φ8	2φ8	1φ8	2φ8	φ8-100	387	3φ10	3φ10	470	2φ8	387
18	DEB-15	27.80	-	2.58	-	1.37	-	2φ8	2φ8	-	3φ8	φ8-100	387	3φ10	3φ10	470	2φ8	387
19	DEB-16	27.80	-	2.58	-	1.37	-	2φ8	2φ8	-	4φ8	φ8-100	387	-	3φ10	470	2φ8	387
20	DEB-17	28.10	-	2.62	-	1.41	-	2φ8	2φ8	1φ8	1φ8	φ8-100	387	3φ10	3φ10	470	2φ8	387
21	DEB-18	27.30	-	2.52	-	1.41	-	-	-	-	3φ8	φ8-100	387	3φ10	3φ10	470	2φ8	387
22	DEB-19	27.30	83.20	2.52	6.37	1.41	4.86	-	-	-	3φ8	φ8-100	387	-	3φ10	470	2φ8	387
23	DEB-20	27.30	82.80	2.52	6.31	1.41	4.81	2φ8	2φ8	-	1φ8	φ8-100	387	-	3φ10	470	2φ8	387
24	DEB-21	27.30	82.80	2.52	6.31	1.41	4.81	2φ8	2φ8	-	3φ8	φ8-100	387	3φ10	3φ10	470	2φ8	387
25	DEB-56	28.40	105.26	2.68	7.84	1.46	5.73	-	-	-	-	φ8-100	387	3φ10	3φ10	470	2φ8	387
26	DEB-57	28.40	105.26	2.68	7.84	1.46	5.73	2φ8	2φ8	3φ8	-	φ8-100	387	3φ10	3φ10	470	2φ8	387
27	DEB-58	28.40	105.26	2.68	7.84	1.46	5.73	2φ8	2φ8	1φ8	2φ8	φ8-100	387	3φ10	3φ10	470	2φ8	387

Table 2 Mix proportions of NSC and ECC.

Ingredients	NSC kg/m ³	ECC-1 kg/m ³	ECC-2 kg/m ³
Ordinary portland cement (C)	450.00	583.00	590.00
Fly ash (FA)	–	700.00	354.00
Silica fume (SF = 10%)	–	–	94.40
Water (W)	261.00	187.32	165.20
Fine aggregate (FnAg)	745.00	467.01	472.00
Coarse aggregate (CAG)	910.00	–	–
Superplasticizer (SP)	–	14.11	15.10
PVA fiber (ECC-1; V _f = 2% and ECC-2; V _f = 1.5%)	–	26.00	19.50

445.67% compared to the DEB-1. This was attributed to the ability of the dapped-end reinforcements to resist the shear force and diagonal cracks that occur in the dapped-end region.

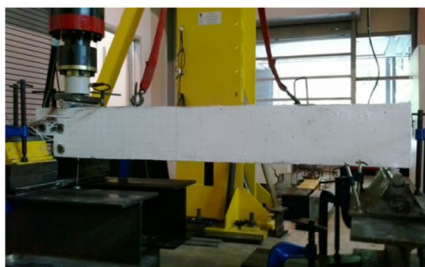
In comparison with the DEB-3, the decrement of the failure load and deflection capacity occurred at the DEB-4, DEB-5, and DEB-7, which were 7.52% and 5.10%, 13.28% and 11.88%, and 20.97% and 20.49%, respectively. This was caused by the reduction of the HR amount used, where the greater the amount of the HR that is reduced, then the greater the reduction in the capacity. It exhibits that the HR has an important role in contributing to the strength and deflection capacity of the DEB.

Table 3 Fresh SC-ECC test results.

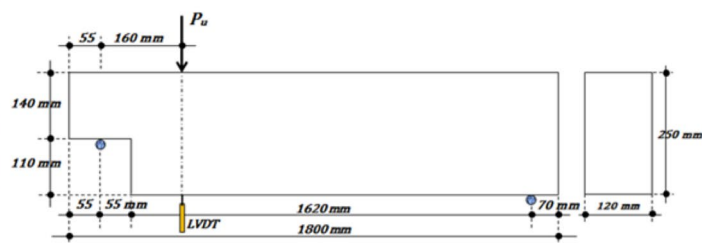
Type	Slump flow		V-funnel	L-box		
	Slump flow diameter (mm)	T500 (s)	t _v (s)	h ₁ (mm)	h ₂ (mm)	h ₂ /h ₁
ECC-1	839	4	8	90	85	0.94
ECC-2	847	4	7	91	87	0.96

Table 4 Mechanical properties of the hardened concrete/ECC.

Mechanical properties	Testing method	Number of samples and size	Unit	Average value of three samples		
				NSC	ECC-1	ECC-2
Compressive strength (<i>f'_c</i>)	ASTM C39/C39M-04	3 cylinders of 100 mm dia. and 200 mm height	MPa	28.48	85.72	105.26
Splitting tensile strength (<i>f'_{sp}</i>)	ASTM C496/C496M-04	3 cylinders of 100 mm dia. and 200 mm height	MPa	2.67	6.42	7.84
Elastic modulus (<i>E</i>)	ASTM C469-02	3 cylinders of 150 mm dia. and 300 mm height	GPa	23.84	36.12	38.09
Poisson ratio (<i>ϑ</i>)	ASTM C469-02	3 cylinders of 150 mm dia. and 300 mm height	–	0.185	0.243	0.257
Flexural strength (<i>S_f</i>)	ASTM C293-02/C293M-04	3 beams of 500 mm × 100 mm × 24 mm	MPa	3.79	11.74	13.42
Direct tensile strength (<i>f_t</i>)	ASTM D2936; ASTM 1992	3 samples with the prism dog bone shape	MPa	1.46	4.88	5.73
Tensile strain capacity (<i>ε_t</i>)	ASTM D2936; ASTM 1992	3 samples with the prism dog bone shape	%	0.15	2.93	4.09
Density of hardened concrete (<i>γ_c</i>)	ASTM C	3 cylinders of 150 mm dia. and 300 mm height	kg/m ³	2327	2243	2248
Permeability (<i>P</i>)	ASTM C1202	3 cylinders of 100 mm dia. and 50 mm height	C	4348	1393	496

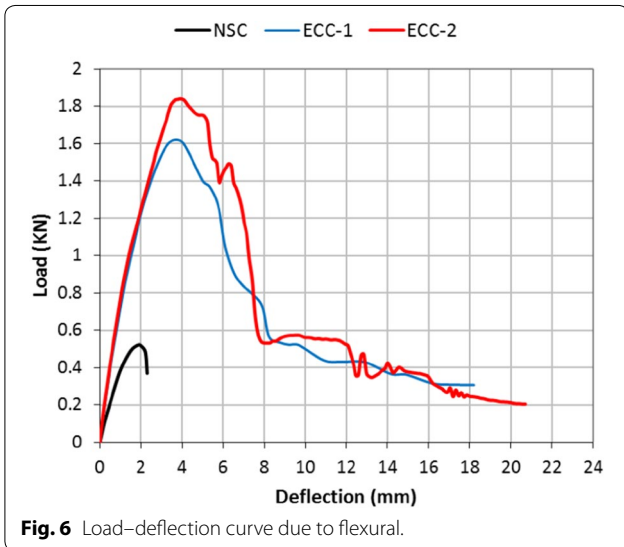
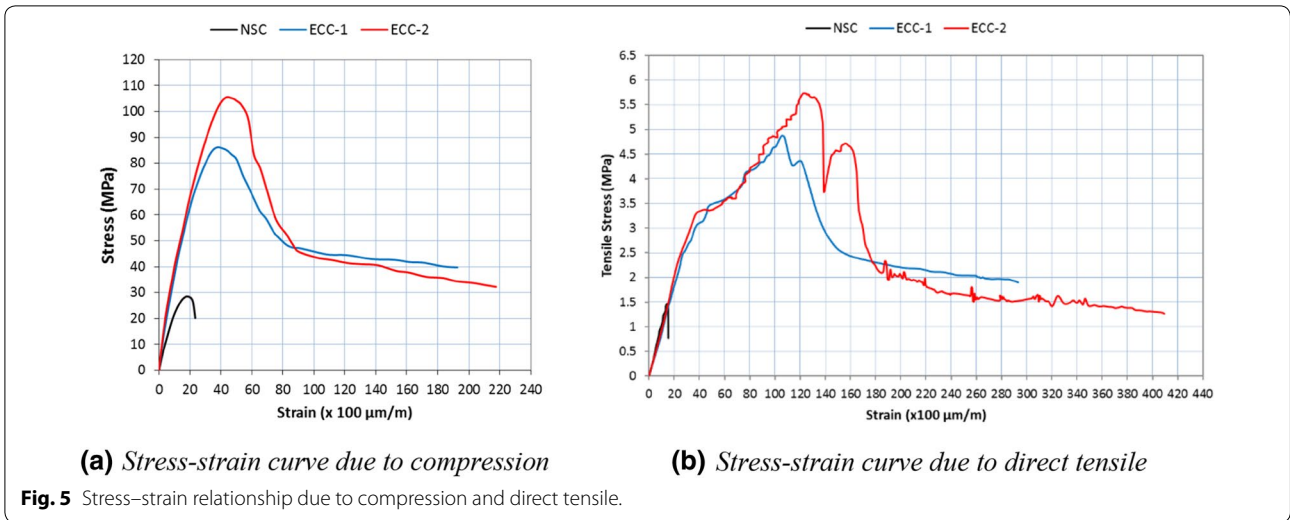


(a) Beam setting at loading frame



(b) Load position, beam and nib size

Fig. 4 Experimental setup of DEB specimen.

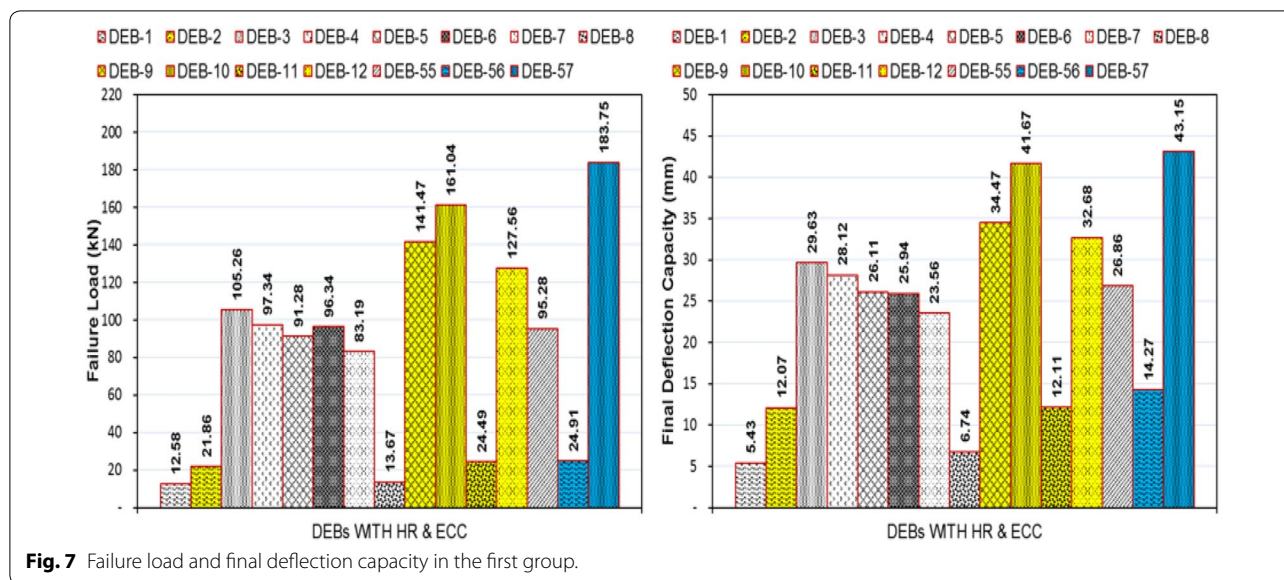


Compared to the DEB-3, the DEB-6 also experienced a decrement in the failure load of 8.47% and deflection capacity of 12.45%. This was due to the excessive amount of the HR in dapped-end region of the DEB-6. This beam used 4Ø8 for the HR, which caused the value of a_n/d to be greater than 1. This value did not meet the PCI requirements. According to PCI code, related equation exhibits that if the value of a_n/d is increased, normally, the amount of the NFR will be increased also. But, in fact, the DEB-6 still used 3Ø10 for the NFR, similar to the DEB-3. This condition caused a significant difference in the strength capacity between the NFR and the HR, where the strength capacity of the HR increased sharply, which was caused by the DEB-6 using 4Ø8. Referring

to the PCI provision, the HR of the DEB-6 was stronger than the NFR and failure occurred first at the NFR whilst for the DEB-3, the first failure occurred at the HR. Accordingly, the capacity of the DEB-6 was lower than the DEB-3.

Actually, the parameter reviewed for the DEB-55 was not directly related to the parameter of this group because the DEB-55 considered variation of BMFR. So in this part, the discussion focused on the use of A_{sh} that was intended for the development of the length of the HR. To meet the proper level of anchorage of the BMFR at the end face, the steel bar number of the BMFR was taken as being equal to A_{sh} . Referring to the design stage, when the BMFR used steel bars of 3Ø10 (or $A_{st} = A_{sh} = 78.125\%$ of A_{sh}), it turns out, the strength capacity of the full-depth beam was larger than the failure load of the DEB-3. So, to meet the analysis requirement, the BMFR (or $A_{st} = A_{sh}$) of the DEB-55 was taken as being less than 3Ø10, that was, 3Ø8. The test result exhibits that the capacity decrement of the DEB-55 occurred on the failure load of 9.48% and deflection capacity of 9.35% compared to the DEB-3. By considering the PCI provision, basically, there was no difference in the strength capacity between the DEB-3 and the DEB-55, causing both DEBs to have the same dapped-end reinforcements. Aside from that, the PCI code also did not specify variation of BMFR clearly. It implies that capacity of DEB can be influenced by the amount of the BMFR used.

The DEB-7 used the dapped-end reinforcements, but without the HR whilst the DEB-8 only used the HR in the dapped-end region and without other dapped-end reinforcements. There was a significant difference in the capacity between the DEB-7 and DEB-8. The capacity



of the DEB-7 was much higher compared to the DEB-8, which had a failure load of 508.56% and deflection capacity of 249.55%. In fact, as occurred at the DEB-8, it has exhibited that the HR cannot act alone to resist the shear force in the dapped-end region. However, at least the NFR or NHR should be involved together with the HR in resisting the shear force in the dapped-end region.

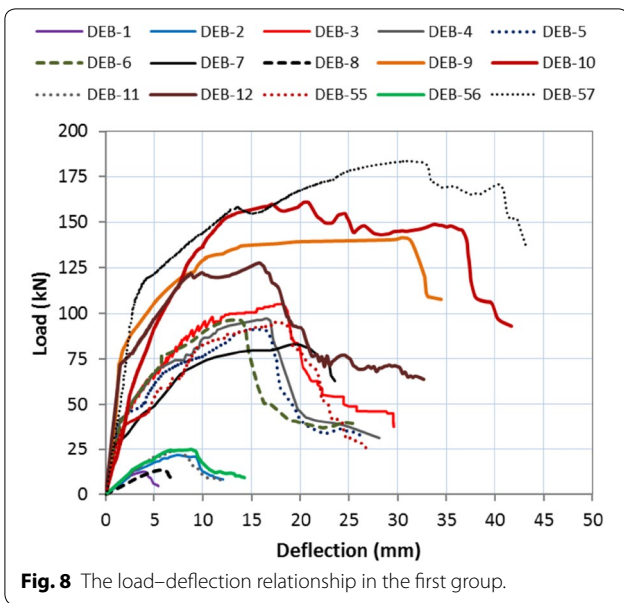
Replacing the NSC with the ECC-1 in the dapped-end region increased the increment of the DEB capacity in both the failure load and final deflection. The enhancement of the failure load and deflection capacity can be described as follows: 73.77% and 122.28% for the DEB-2 compared to the DEB-1, 52.99% and 40.63% for the DEB-10 in comparison to the DEB-3. Further, an increment on the failure load of 54.98% and on the final deflection of 32.02% was achieved by the DEB-9 compared to the DEB-5. In the meantime, by comparing the DEB-12 against the DEB-7, as well as the DEB-11 to the DEB-8, the increment on the failure load and final deflection capacity can be described as follows: 53.34% and 38.71% for the DEB-12, as well as 79.15% and 79.67% for the DEB-11. Referring to the mechanical properties results, the ECC-1 was superior compared to the NSC. Accordingly, the ECC-1 can improve the failure load and final deflection capacity of the DEB. There was strong bonding between the steel bars and the ECC-1. In addition to that, the ECC-1 had a strain capacity up to 2.93% whilst the yield strain of the steel bar was around 0.226%; moreover, the ECC-1 could still do the plastic deformation even though the steel bars had passed their yield strain phase.

According to their mechanical properties, the ECC-2 was better than the ECC-1. The increment of the failure load and deflection capacity for the DEB-56 against the

DEB-2 was 13.95% and 18.23% whilst for the DEB-57 compared to the DEB-10, it was 14.10% and 3.55%. The higher strength of the ECC-2 was achieved by better micro-filling and more pozzolanic effect due to the use of silica fume (SF) that had a high fineness particle size and was rich in SiO₂. In addition, the oiled surface treatment of the PVA fibers in the ECC-2 provided a better ductility effect compared to the ECC-1. The above evidences have proved that the R-ECC-DEBs have a higher capacity than the RC-DEBs.

3.4 The Load–Deflection Relationship, Crack Pattern and Failure Mode in the First Group

Behavior of DEB specimens in the pre-peak and post-peak ranges can be observed and understood based on curve of load–deflection relationship. The load–deflection relationships of the DEB-1, DEB-3, DEB-4, DEB-5, and DEB-7 in the first group are given in Fig. 8. DEB-1 showed inadequate behavior where DEB-1 was subjected to a sudden rupture after reaching its peak load. Aside from that, DEB-1 was characterized by the lowest capacity in the failure load and final deflection. The DEB-3, DEB-4, and DEB-5 exhibited similar behavior in pre-peak range, but in post-peak range, behavior of DEB-5 exhibited a decline, as there was no capability to withstand the applied load. However, the DEB-5 still had the ability to perform more plastic deformation up to failure. On the other hand, for the DEB-7, the absence of the HR causes a significantly different behavior compared to the DEB-3, DEB-4, and DEB-5. In the post-peak range, once the DEB-7 reached its peak load, no large plastic deformation was generated.



DEB-1 as a reference beam experienced the failure quite fast. The first cracking emerged from re-entrant corner at load of 6.48 kN. Once it reached the first cracking load, the crack propagated fast and diagonally towards the load point and achieved the ultimate load of 21.86 kN; furthermore, the beam failure took place quickly. The ability of DEB-1 to withstand the shear force was only supported by the concrete. The failure of DEB-1 was indicated by the dominant diagonal crack emanating from re-entrant corner as shown in Fig. 9.

The DEB-3, DEB-4, and DEB-5 had much better behavior compared to the DEB-1. The dapped-end

reinforcements were able to resist the diagonal cracks occurring in the dapped-end region. The first cracking of all these beams appeared from the re-entrant corner. Initially, this crack propagated diagonally, but the propagation of this crack was inhibited and resisted by the HR. Therefore, during the loading, other cracks also emerged at the support. When the applied load increased, the cracks at the support developed and propagated towards the load point upwards to reach the ultimate load, and finally, reached their rupture point. For the DEB-3, the failure condition was indicated by the dominant diagonal crack at the support and the diagonal crack at the re-entrant corner. In the meantime, for the DEB-4 and DEB-5, the failure condition was characterized by the dominant diagonal cracks at the re-entrant corner, at the support, and at the corner of the dapped-end. Severe damage occurred at the dapped-end region due to the reduction in the steel bars of the HR, with the DEB-4 or DEB-5. In addition, the flexural moment generated by the vertical shear force at the support caused the dominant diagonal cracks and severe damage of the dapped-end section.

The failure condition of all these beams can be seen in Fig. 9. However, for the DEB-7, the failure load and final deflection capacity were lower than the DEB-3, DEB-4, and DEB-5. The absence of the HR influenced its capacity and behavior. Basically, there were two effects produced due to the absence of the HR. Firstly, the diagonal crack from the re-entrant corner developed and propagated towards the load point. During the loading, this crack was resisted by the NFR and the NHR. Secondly, the flexural moment caused the diagonal crack to propagate along the NFR up to failure. Therefore, the capacity of

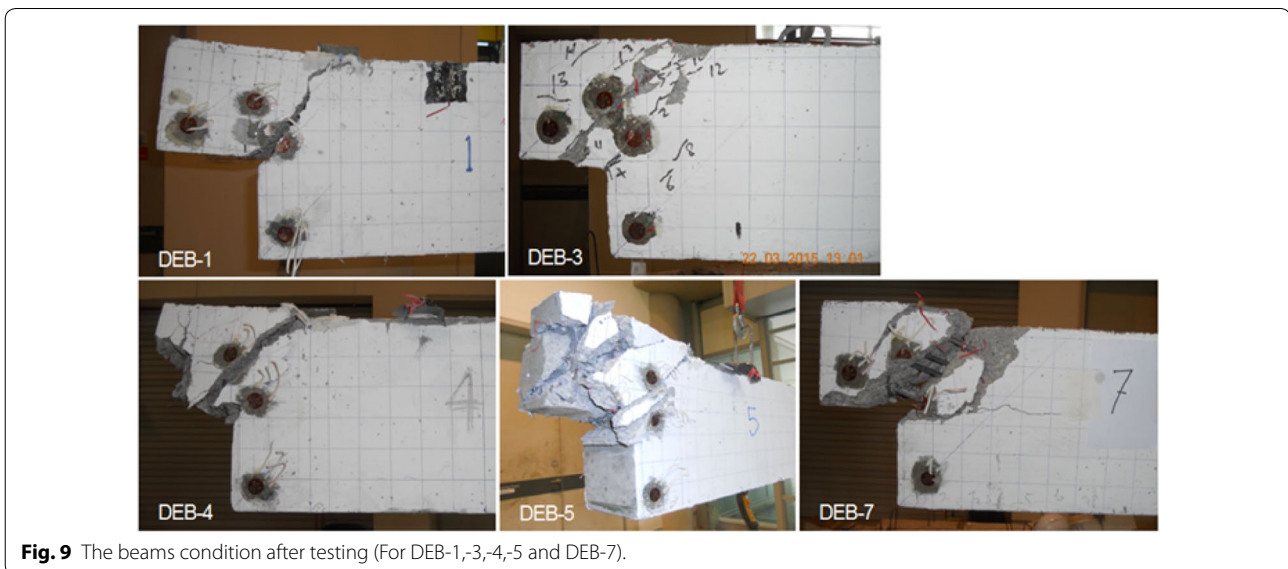




Fig. 10 The beams condition after testing (For DEB-6 and DEB-55).



Fig. 11 The beam condition after testing (For DEB-8).

the DEB-7 is not drop significantly even without the HR. The failure condition of the DEB-7 was indicated by the severe damage at the re-entrant corner. All of the beams above failed in the shear failure mode.

The load–deflection relationships of the DEB-6 and DEB-55 in the first group are given in Fig. 10. The DEB-55 exhibited a similar behavior to DEB-3 in the pre-peak and post-peak ranges, but the behavior of the DEB-6 exhibited a decline after reaching the post-peak, as if it had no capability to withstand the applied load. The DEB-6 still had the ability to conduct more plastic deformation up to the failure. The variations of the HR caused the changes of the behavior of the DEB specimens.

Basically, the DEB-6, DEB-55, and DEB-3 had similar crack patterns and failure modes. The first cracking of the beams emerged from the re-entrant corner. Initially, the crack propagated diagonally, but the HR of all these beams was able to inhibit and resist the diagonal crack from the re-entrant corner. Accordingly, other cracks also appeared at the support during the beam loading. The cracks at the support developed when the applied load increased and the cracks propagated toward the load point up to the rupture. The failure condition of these beams was characterized by the dominant diagonal crack at the support, as well as the diagonal crack at the re-entrant corner. The DEB-6 and DEB-55 failed in the shear failure mode.

There was a significant difference in the beam behavior between the DEB-7 and DEB-8 as shown in Figs. 9 and 11. During the beam loading, the first cracking of both beams appeared at the re-entrant corner. Basically, the HR was able to resist the diagonal crack emanating from the re-entrant corner, but in fact, the absence of the HR in the DEB-7 did not provide a large effect in reducing the capacity of the beam. The NFR or NHR also has the ability to resist the diagonal crack or shear force. Therefore, the DEB-8 that only used the HR (without other dapped-end reinforcements) exhibited a lower capacity compared to the DEB-7. The DEB-8 did not have the NFR to resist the flexural moment caused by the vertical shear force at the support. Accordingly, the DEB-8 only improved a little on the capacity compared to the DEB-1. According to Fig. 11, for the DEB-8, initially, the diagonal crack emerged from the re-entrant corner, but this crack could not propagate diagonally because it was resisted by the HR. Due to the absence of the NFR and NHR, this crack propagated in a vertical direction parallel to the direct shear plane. The failure process of the beam took place in a short time and failed in the shear failure mode. The HR could not work alone to improve the performance of the DEB. This condition has proved that the existence of the HR should be supported by the NFR or NHR to achieve better performance of the DEB.

It has been exhibited, aforementioned, that the ECC-1 can improve the failure load and final deflection of the DEB. Figure 12 shows the behavior comparison between the DEB-1 and DEB-2, DEB-3 and DEB-10, DEB-5 and DEB-9, DEB-7 and DEB-12, as well as the DEB-8 and DEB-11. According to this comparison, the behavior of the R-ECC-DEBs was better than the RC-DEBs. In the post-peak range, the R-ECC-DEBs can develop large plastic deformations up to failure. According to the observation during the beam testing, in general, the failure process of the R-ECC-DEBs took a longer time than the RC-DEBs.

In the previous section, the crack pattern and failure condition of the DEB-1, DEB-3, DEB-5, DEB-7, and

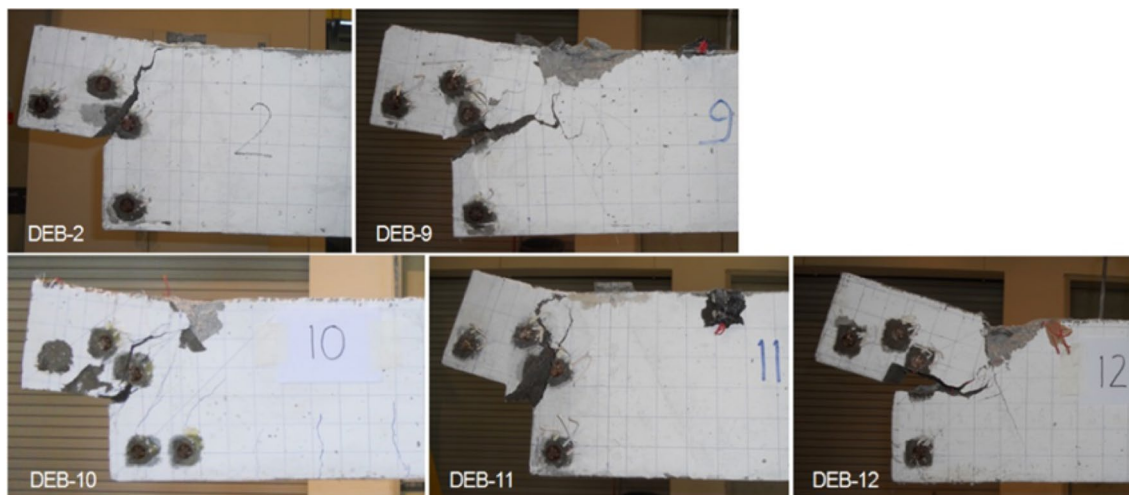


Fig. 12 The beam condition after testing (For DEB-2,-9,-10,11 and DEB-12).

DEB-8 were shown. As shown in Fig. 12, the failure condition of the DEB-2 was similar to the DEB-1, and the DEB-11 was similar to the DEB-8. Due to the use of the ECC-1, for the DEB-9 and DEB-10, the bonding strength between the ECC-1 with the NFR was stronger than the HR so the weak point moved to the HR. The flexural moment caused a dominant crack to occur at the re-entrant corner. However, for the DEB-12, the strong bonding between the ECC-1 and NFR was able to resist the diagonal crack from the support and the re-entrant corner, but due to the flexural moment, de-bonding occurred along the NFR measured from the center of the flexural moment. The first cracking of all of the above beams occurred at the re-entrant corner. In comparison with the RC-DEBs, for the R-ECC-DEBs, there was no spalling occurring but the cracks were wider. The crack propagation was longer and clearer. Some fine cracks always accompany the dominant cracks. All these beams failed in the shear failure mode, but on the DEB-10, some flexural cracks appeared at the soffit of the main beam. It

indicates that the ECC played an important role in contributing to the adequate capacity and behavior of the dapped-end beams.

Figure 13 shows the superiority of the ECC-2 that was used for the DEB specimens compared to the ECC-1 which involved a comparison between the DEB-56 and DEB-2, as well as the DEB-57 and DEB-10. Due to the use of the ECC-2, there were some improvements generated which covered the failure load and final deflection capacity. Basically, their behaviors were quite similar, either in the pre-peak or post-peak range. Likewise, with the crack pattern and failure condition of these two R-ECC-DEBs, there was a slight difference between them. For the DEB-57, at the failure condition, Aside from at the re-entrant corner, the dominant diagonal crack also occurred at the support. Due to the use of the ECC-2, the center point of the flexural moment was stronger than the region in between this point and the support. The flexural effect at this region caused the dominant diagonal crack to occur at the support. The first cracking of the DEB-56 and



Fig. 13 The beam condition after testing (For DEB-56 and DEB-57).

DEB-57 was initiated from the re-entrant corner. Both the R-ECC-DEBs failed in the shear failure mode. During testing of the DEB-57, it was observed that some fine flexural cracks appeared at the soffit of the main beam, but after the loading stopped, these cracks were not visible. All of the above evidences have exhibited that the performance of the R-ECC-DEBs was better than the RC-DEBs.

3.5 The Failure Load and Final Deflection Capacity for the Beams in the Second Group

Figure 14 shows the test results of all the DEB specimens in the second group. The variation of the DR provided the changes of the failure load and final deflection capacity of the DEB specimens.

The DEB-15 was derived from the DEB-3, where all of the vertical HRs were replaced by the DR. By comparing the DEB-15 with the DEB-3, the existence of the DR significantly improved the failure load and final deflection capacity of the DEB by 21.09% and 10.50%, respectively. The DRs were placed with an inclination of around 45° to the longitudinal axis. This position provided an advantage for the DR in resisting the tensile force that acted perpendicular to the crack. Therefore, the DR was able to withstand the tensile force adequately compared to the vertical HR. Due to this condition, the DEB-15 had a higher capacity than the DEB-3.

In comparison with the DEB-15, the decrement of the failure load and deflection capacity occurred at the DEB-14 and DEB-13, they were 9.40% and 7.88%, and 20.54% and 15.33%, respectively. It was caused by the reduction of the DR amount used, where the more DR that was

reduced then, the greater the reduction in the capacity. The DR had a significant effect on the contribution of the strength and deflection capacity. In addition, if compared to the DEB-15, The DEB-16 also experienced a decrement of the failure load of 7.01% and deflection capacity of 14.84%. It was caused by the additional DR amount. In this case, the excessive amount of the DR was able to cause the decrement in capacity of the DEB.

This situation was similar to the case of the DEB-6 in the previous section. The nominal shear span (a_n) was determined in an analogue way. Owing to the DEB-16 using 4Ø8 for its DR, the value of a_n/d was greater than 1. This value was not in accordance with the PCI provision. According to PCI code, the design equation exhibits that if the value of a_n/d increased, normally, the amount of the NFR would be increased also. But, in fact, the DEB-16 continued to use 3Ø10 for the NFR. This condition caused a significant difference in the strength capacity between the NFR and DR, where the strength capacity of the DR becomes larger due to using of the closed stirrup of 4Ø8. The failure may have occurred at the NFR. Therefore, the capacity of the DEB-16 was lower than the DEB-15.

The DEB-13 used 1Ø8 for its DR, but without the HR; in the meantime, the DEB-17 was derived from the DEB-13 by adding 1Ø8 for the HR, whilst the DEB-14 utilized the DR of 2Ø8 without the HR, and the DEB-14A was created from the DEB-14 by adding 1Ø8 for the HR. In comparison with the DEB-13, the DEB-17 had an increment on the failure load of 19.54% and final deflection of 12.66%, whilst the DEB-14A provided an increment on the failure load of 16.57% and final deflection of 9.91%.

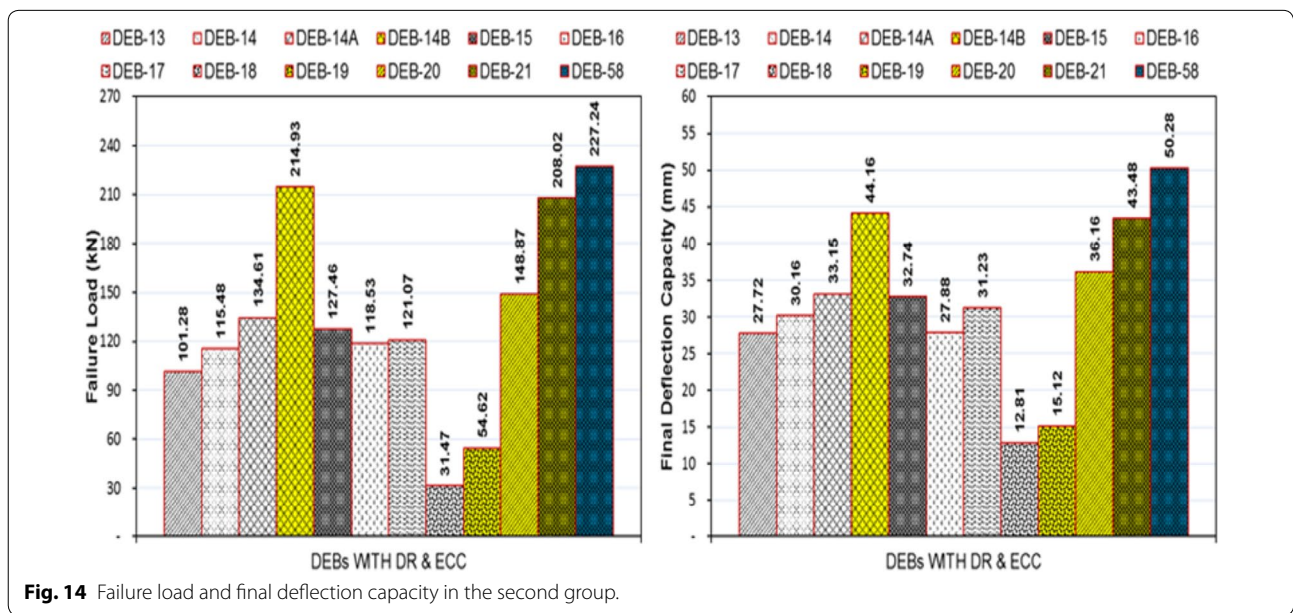


Fig. 14 Failure load and final deflection capacity in the second group.

There was an increment of the capacity for the DEB-17 and DEB-14A by adding the HR of 1Ø8 only. It has been proved that the combination of the HR and DR can contribute to and improve the capacity of the DEB specimens.

By using the ECC-1 placed in the dapped-end region, it has been proved that the increment of the DEB capacity occurred for both the failure load and final deflection, as shown in Fig. 14. The enhancement of the failure load and final deflection capacity can be described as follows: 73.56% and 18.03% for the DEB-19 compared to the DEB-18, 46.99% and 30.45% for the DEB-20 compared to the DEB-13, 59.67% and 33.21% for the DEB-14B compared to the DEB-14A, as well as 63.20% and 32.80% for the DEB-21 compared to the DEB-15. The ECC-1 improved the capacity of the DEB on the failure load and final deflection. It was attributed to the strong bonding between the steel bars and the ECC-1. In addition to that, the ECC-1 performed the plastic strain up to 2.93% even though the steel bars had passed their yield strain phase, where the yield strain of the steel bars was around 0.226%.

By considering the DEB-14A, DEB-14B, and DEB-58, where all of these beams had the same reinforcement scheme, the ECC-2 provided the DEB-58 with a higher capacity compared to the DEB-14B that used the ECC-1. Compared to the DEB-14B, the DEB-58 had an increment of the failure load of 5.73% and final deflection capacity of 13.86%. The higher strength of the ECC-2 was caused by the better micro-filling and more pozzolanic effect due to the use of the silica fume (SF) that had a high fineness particle size and was rich in SiO₂. In

addition to that, the oiled surface treatment of the PVA fibers in the ECC-2 had provided a better ductility effect compared to the ECC-1. However, the above evidences have proved that the R-ECC-DEBs had a higher capacity than the RC-DEBs.

There was a different capacity between the DEBs using the HR and the DR as shown in Fig. 15. Based on the charts, all of the DEBs with the DR had a higher capacity compared to the DEBs with the HR. The increment on the failure load and final deflection capacity can be reported as follows: 10.96% and 6.17% for the DEB-13 compared to the DEB-5, 18.64% and 7.25% for the DEB-14 compared to the DEB-4, 21.09% and 10.50% for the DEB-15 compared to the DEB-3, 23.03% and 7.48% for the DEB-16 compared to the DEB-6, 130.21% and 90.06% for the DEB-18 compared to the DEB-8, 123.03% and 24.86% for the DEB-19 compared to the DEB-11, 5.23% and 4.90% for the DEB-20 compared to the DEB-9, as well as 29.17% and 4.34% for the DEB-21 compared to the DEB-10.

3.6 The Load–Deflection Relationship, Crack Pattern and Failure Mode in the Second Group

The behavior of the DEB specimens in the pre-peak and post-peak ranges can be observed and understood based on the curve of the load–deflection relationship. The load–deflection relationships of the DEB-15, DEB-14, DEB-13, and DEB-16 in the second group are given in Fig. 16. Basically, the DEB-15, DEB-14, DEB-13, and DEB-16 exhibit similar behavior in the pre-peak range to the DEB-3, but in the post-peak range, the behavior of the DEB-13 was similar to the DEB-3, where their curve

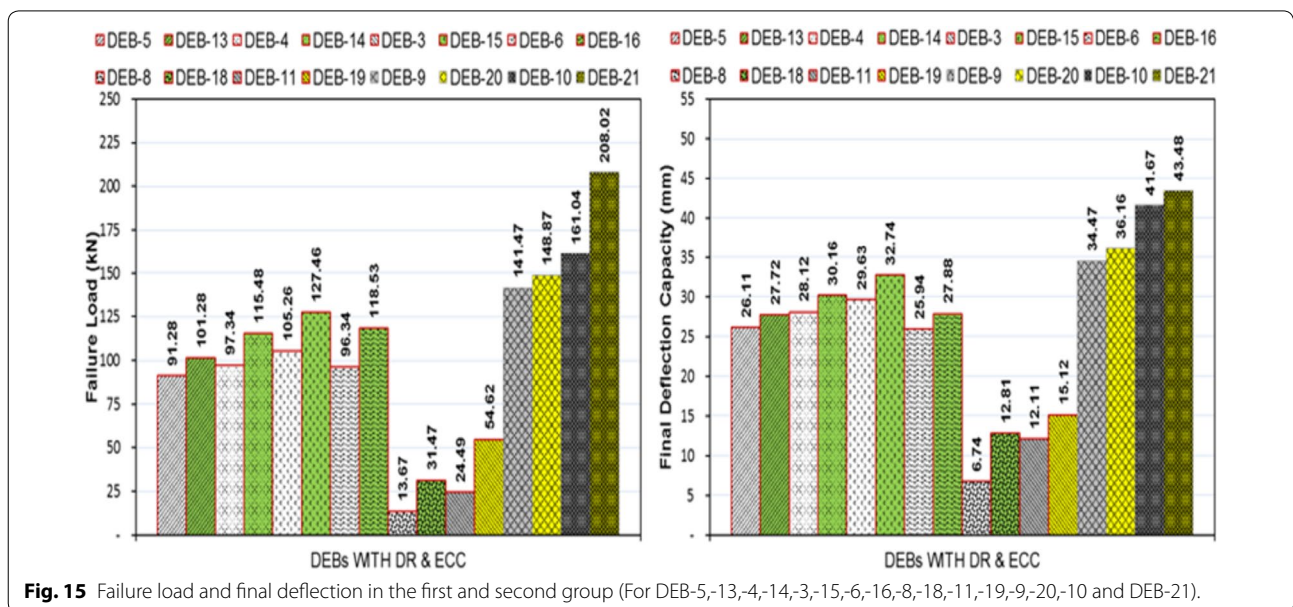
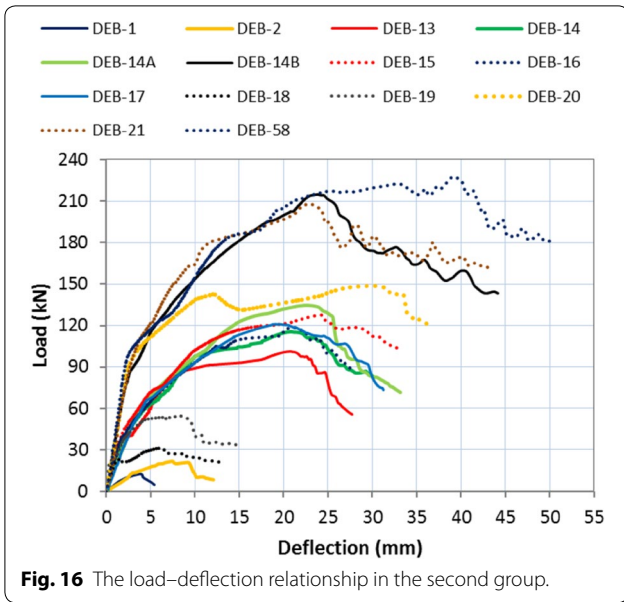


Fig. 15 Failure load and final deflection in the first and second group (For DEB-5,-13,-4,-14,-3,-15,-6,-8,-18,-11,-19,-9,-20,-10 and DEB-21).



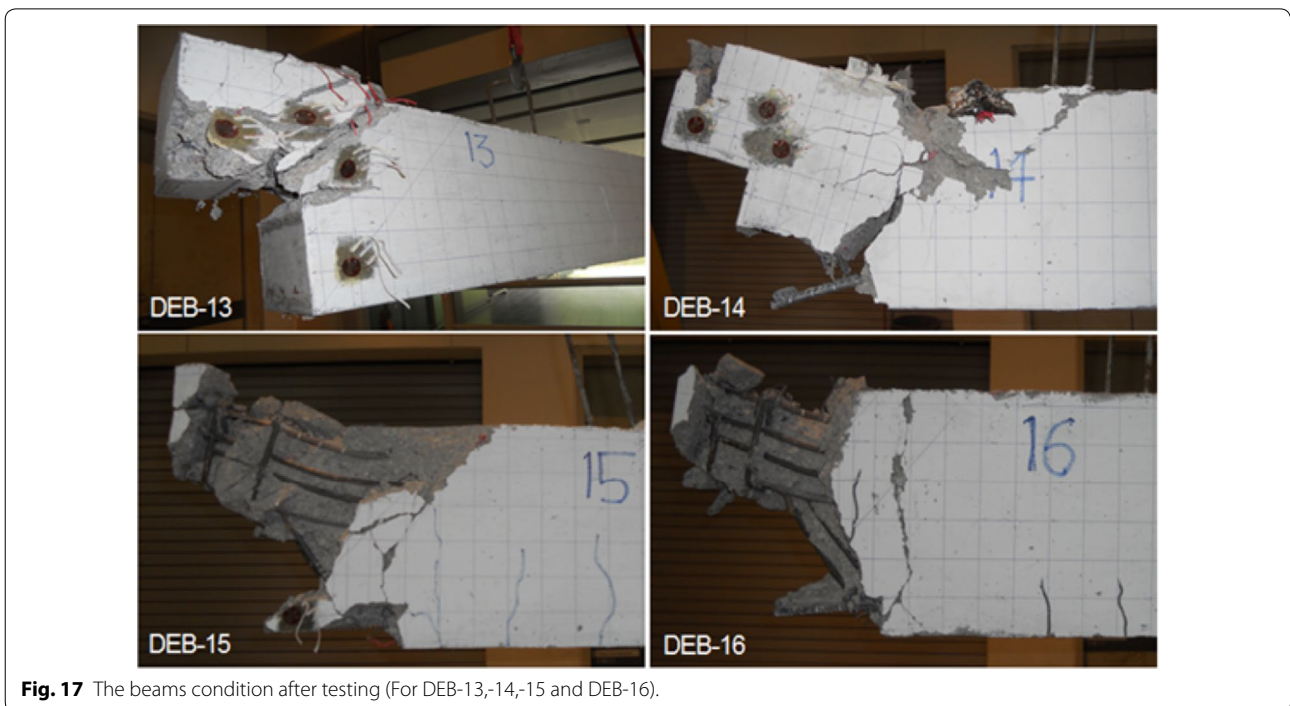
exhibits a decline and rather steeply. On the other hand, for the DEB-15, DEB-14, and DEB-16, their softening effect was more dominant compared to the DEB-3 and DEB-13. However, the DEB-15 exhibits the ability to perform more plastic deformation up to failure compared to other beams.

Related to the DEB-14, DEB-15, and DEB-16, adequate amounts of the DR in the dapped-end region

provided a sufficient capacity for the DEB. The DR of these beams had enough ability to resist the diagonal crack in the dapped-end region. But, due to the absence of the HR, there was no confinement strength to resist the diagonal crack emanating from the un-dapped portion. This area became the weakest point of the DEB. The above condition caused the DEB-14, DEB-15, and DEB-16 to fail in the un-dapped region.

This was contrary to the DEB-13, where this beam used 1Ø8 only for the DR. Its DR was unable to resist, adequately, the diagonal cracks or shear force in the dapped-end region. As a result, diagonal cracks from the re-entrant corner and the support developed and propagated to the load point up to failure. The failure condition of the DEB-13 was indicated by the dominant diagonal cracks occurring at the re-entrant corner and at the support. The first crack of all of the above beams emerged at the re-entrant corner. The DEB-13 failed in the shear failure modes whilst the DEB-14, DEB-15, and DEB-16 failed in the shear-flexural mode due to some flexural cracks appearing at the soffit of the main beam (Fig. 17).

The existence the HR of 1Ø8 mm in the dapped-end region of the DEB specimen with the DR improved the behavior of the DEB both in pre-peak and post-peak ranges. The DEB-17 reached the ultimate load and final deflection with a higher load than the DEB-13, likewise for the DEB-14A compared to the DEB-14 as shown in Fig. 18.



By adding 1Ø8 mm of the HR in the DEB-14A and DEB-17, the HR in these beams was able to contribute to the confinement strength at the end face of the beam so that the HR was able to, adequately, resist the diagonal crack from the corner of the un-dapped portion. During the testing, it was observed that the first cracking emerged from the re-entrant corner. The existence of the HR and the DR inhibited or helped to avoid the propagation of this crack, therefore, other cracks appeared at the support and its vicinity. These cracks developed and propagated to the load point up to failure. The failure condition of these beams was characterized with a dominant diagonal crack at the support and severe damage.

It has been explained, aforementioned, that the failure load and final deflection of the DEB can be improved by using the ECC-1 or the ECC-2. Figure 19 shows the comparison of the behavior between the DEB-18 and DEB-19, the DEB-13 and DEB-20, the DEB-14A and DEB-14B, the DEB-14B and DEB-58, as well as the DEB-15 and DEB-21. The behavior of the R-ECC-DEBs was better than the RC-DEBs. In the pre-peak range, the R-ECC-DEBs slowed down the occurrence of the first crack; whilst in

the post-peak range, the R-ECC-DEBs developed large plastic deformations up to failure. Generally, according to the observation during the beam testing, the failure process of the R-ECC-DEBs took a longer time than the RC-DEBs.

In the previous section, the crack pattern and failure condition of the DEB-18, DEB-13, DEB-14A, and DEB-15 were shown. Figure 19 can be utilized to compare the failure condition between the DEB-19 and DEB-18, the DEB-20 and DEB-13, the DEB-14B and DEB-14A, as well as the DEB-21 and DEB-15. The first crack of all the above beams was always initiated from the re-entrant corner. Even though using different concrete types, the DEB-19 and DEB-18 exhibited similar crack patterns and failure modes. The DR had the ability to resist the diagonal crack from the re-entrant corner, but then the crack emerged at the support. The vertical shear force at the support acted dominantly causing cracks to develop and propagate vertically up to failure. With the DEB-20, the ECC-1 provided strong bonding on the dapped-end reinforcements. Initially, the cracks propagated diagonally. Due to the bonding strength between the ECC-1



Fig. 18 The beams condition after testing (For DEB-14A and DEB-17).

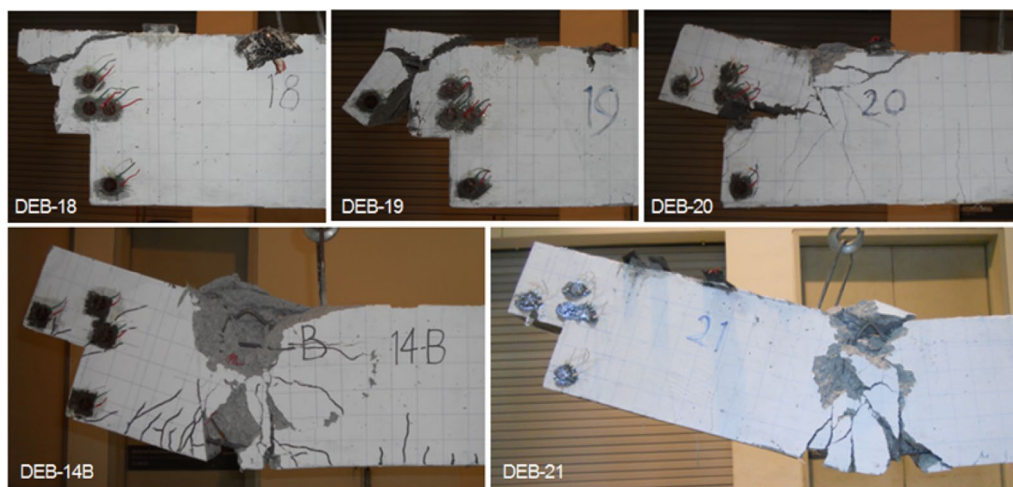


Fig. 19 The beams condition after testing (For DEB-18,-19,-20,-14B and DEB-21).

against the NFR and the DR, the center point of the flexural moment was the weakest point. Due to the flexural moment, a diagonal crack from the re-entrant corner appeared and developed. During the beam loading, delaminating occurred between the ECC-1 and the NFR measured from the center point. The crack propagated horizontally along the NFR up to the failure. Some of the flexural cracks appeared at the soffit of the main beam; therefore, the failure of the DEB-20 can be categorized as the shear-flexural failure mode.

The DEB-14B was the R-ECC-DEB derived from the DEB-14A. As shown in Fig. 19, the ECC-1 provided a significant increment on the failure load and final deflection capacity of the DEB-14B. The combination between the ECC, DR, HR, and other dapped-end reinforcements generated adequate performance on the DEB-14B. This beam had a high failure load capacity and also performed large plastic deformations. The dapped-end region of the DEB-14B was very strong. The dapped-end section was able to resist the shear force and diagonal cracks that occurred. Finally, the DEB-14B failed in the flexural mode. Many flexural cracks occurred at the soffit of the main beam. In addition, the DEB-21 had a similar case to the DEB-14B. The DEB-21 also failed in the flexural mode as shown in Fig. 19 but the failure location was close to mid-span. The DEB-21 was derived from the DEB-15. Even though only using the NSC, the DEB-15 showed sufficient performance. This was due to the use of the DR in the dapped-end region of the DEB-15. Its failure had also been indicated by some flexural cracks. Based on this fact, the DEB-21 was created, where the ECC-1 was placed in the dapped-end region of the DEB-15. The ECC-1 was superior compared to the NSC. However, the R-ECC-DEBs exhibited better structural performance than the RC-DEBs.

Figure 20 shows the behavior of the DEB-58 that used the ECC-2, as well as the DEB-14B and DEB-21 which utilized the ECC-1 as shown in Fig. 19. There were no improvements generated covering the failure load and final deflection capacity. Basically, their behaviors were quite similar, either at the pre-peak or post-peak ranges. Likewise, with the crack pattern and failure condition of these two R-ECC-DEBs, there was a slight difference in between as shown in Figs. 19 and 20.

For the DEB-58, the failure location was close to mid-span. The ECC-2 was superior compared to the ECC-1 as explained, aforementioned. It caused the DEB-58 to support a higher failure load and final deflection capacity than the DEB-14B or the DEB-21. The DEB-58 also performed larger plastic deformations compared to the DEB-14B or the DEB-21. Nevertheless, all three of these beams failed in the flexural mode. Even though the failures were in the flexural mode, the first crack of these

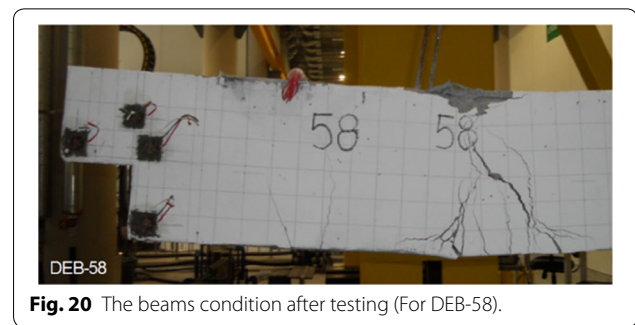


Fig. 20 The beams condition after testing (For DEB-58).

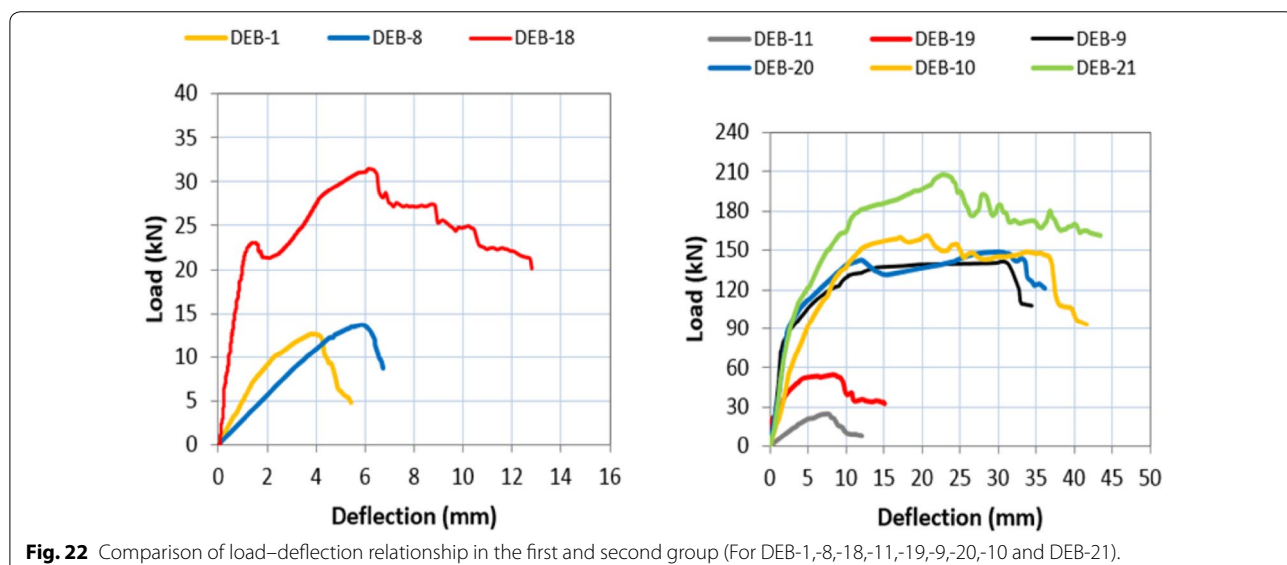
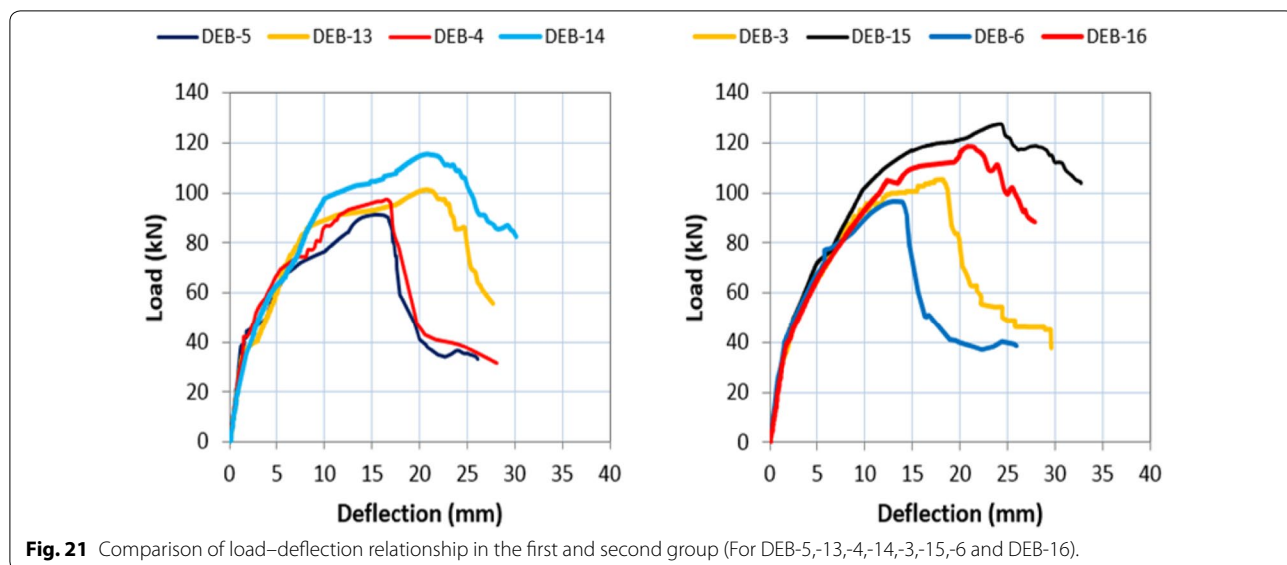
beams (DEB-14B, DEB-21, and DEB-58) were initiated from the re-entrant corner, but this crack was quite fine. The diagonal crack did not develop. After the beams reached their failure, this crack was not visible. The above evidences have exhibited that the structural performance of the R-ECC-DEBs was better than for the RC-DEBs.

As shown in Figs. 21 and 22, all of the DEB specimens that used the DR exhibited a higher capacity compared to the ones using the HR. The proper layout of the DR in the dapped-end region provided an advantage on the capacity of the DEB. The DR which was placed perpendicular to the diagonal crack direction resisted the tensile force more adequately as compared to vertical HR. Basically, the inclination position of the DR provided two positions, which were vertical and horizontal, in the dapped-end region. Definitely these two positions generated different functions/roles. The vertical position can be approximated to have the ability to resist the diagonal crack from the re-entrant corner as the HR whilst the horizontal position may be estimated to have the ability to withstand the flexural moment and the direct shear. The above evidences can be referred to and understood simply, where the DR can improve, significantly, the performance of the DEBs. According to Figs. 21 and 22 both beams that were compared had similar behavior in the pre-peak range, but the beams that used the DR showed better behavior in the post-peak range. Their curves did not fall down, but rather they walked down with ramps up to the point of failure.

4 Conclusion

The following conclusions can be drawn from this study:

1. The first crack is always initiated from re-entrant corner for all dapped-end beams.
2. Diagonal reinforcement (DR) is more appropriate to be used than HR in resisting the diagonal cracks, owing to DR placed in perpendicular to crack direction. Based on test results, use of DR in dapped-end region provides increment for failure load of 40.79%



- and deflection of 24.29% compared to DEB which use vertical HR.
- The DEBs which use DR (without HR) has experienced the severe damage at bottom of un-dapped portion compared to the DEBs that use combination DR with HR. This is due to the related DEBs lose their confinement strength at un-dapped zone.
 - The ECC-1 that was placed in the dapped-end region was able to improve the capacity of the R-ECC-DEBs, where there was an average increment on the failure load of 59.97% and final deflection capacity of 46.67% compared to the RC-DEBs. In the meantime, R-ECC-DEBs that used ECC-2, it exhibited an

- average increment on the failure load of 11.26% and final deflection capacity of 11.88% compared with the R-ECC-DEBs that utilized ECC-1.
- By combining between ECC and the appropriate steel reinforcement configuration, some R-ECC-DEBs can fail in the flexural mode with a higher structural performance.

5 Highlights

- ECC is categorized as ductile composite and high strength capacity.

2. ECC placed in dapped-end region can improve the structural performance of DEBs.
3. The use of diagonal reinforcements is more appropriate than hanger reinforcements.
4. Some of DEBs can fail in the flexural failure mode

Acknowledgments

The authors would like to thank the Ministry of Education (MOE) of Malaysia and Universiti Teknologi PETRONAS for granting the project under code FRGS 2013-2, FRGS 2014-1 and STIRF 38/2012, respectively.

Authors' contribution

BSM has designed the experimental program and helped in the analysis. MA has carried out the experimental work, run the analysis and prepared the first draft of the paper. MSL has helped in the analysis and manuscript proofreading. NAWAZ has helped in the analysis and finalizing the paper. All authors read and approved the final manuscript.

Compliance with ethical standards

Competing interests

The authors declare that they have no competing interests.

Author details

¹ Department of Civil and Environmental Engineering, Universiti Teknologi PETRONAS, 32610 Bandar Seri Iskandar, Perak Darul Ridzuan, Malaysia. ² Departemen Teknik Sipil, Universitas Sumatera Utara, Medan, Indonesia.

Received: 2 April 2019 Accepted: 27 June 2019

Published online: 02 September 2019

References

- A. Committee and I. O. f. Standardization. (2008). Building code requirements for structural concrete (ACI 318-08) and commentary.
- Ahmad, S., Elahi, A., Hafeez, J., Fawad, M., & Ahsan, Z. (2013). Evaluation of the shear strength of dapped ended beam. *Life Science Journal*, *10*, 1038–1044.
- Aswin, M., Mohammed, B. S., Liew, M., & Imam, Z. S. (2015a). Root cause of reinforced concrete dapped-end beams failure. *International Journal of Applied Engineering Research*, *10*(22), 42927–42933.
- Aswin, M., Mohammed, B. S., Liew, M., & Syed, Z. I. (2015b). Shear failure of RC dapped-end beams. *Advances in Materials science and engineering*, *2015*, 309135.
- Botros, A. W., Klein, G. J., Lucier, G. W., Rizkalla, S. H., & Zia, P. (2017). Dapped ends of prestressed concrete thin-stemmed members: Part 1, experimental testing and behavior. *PCI Journal*, *62*, 61–82.
- Desnerck, P., Lees, J. M., & Morley, C. T. (2016). Impact of the reinforcement layout on the load capacity of reinforced concrete half-joints. *Engineering Structures*, *127*, 227–239.
- Forsyth, M. B. (2013). *Behavior of prestressed, precast concrete thin-stemmed members with dapped ends*. Raleigh: North Carolina State University.
- Fu, Z. (2004). *Use of fibres and headed bars in dapped end beams*. Montreal: McGill University Libraries.
- Fukuyama, H., Sato, Y., Li, V. C., Matsuzaki, Y., & Mihashi, H. (2000). Ductile engineered cementitious composite elements for seismic structural applications. In *CD Proceedings of the 12 WCEE, Paper*, 1672.
- Herzinger, R. (2008). *Stud reinforcement in dapped ends of concrete beams*. Ottawa: Library and Archives Canada.
- Herzinger, R., & Elbadry, M. (2007). Alternative reinforcing details in dapped ends of precast concrete bridge girders: experimental investigation. *Transportation Research Record: Journal of the Transportation Research Board*. <https://doi.org/10.3141/2028-13>.
- Huang, P.-C. (2000). Dapped-end strengthening of precast prestressed concrete double tee beams with FRP composites. *Advances in Structural Engineering*, *9*(2), 293–308.
- Huang, P.-C., & Nanni, A. (2006). Dapped-end strengthening of full-scale prestressed double tee beams with FRP composites. *Advances in Structural Engineering*, *9*, 293–308.
- Lepech, M. D., & Li, V. C. (2008). Large-scale processing of engineered cementitious composites. *ACI Materials Journal*, *105*, 358.
- Li, V. C. (1993). From micromechanics to structural engineering—the design of cementitious composites for civil engineering applications. *JSCCE Journal of Structural Mechanics and Earthquake Engineering*, *10*(2), 37–48.
- Li, V. C. (2008). Engineered cementitious composites (ECC) material, structural, and durability performance, Chapter 24. In E. Navy (Ed.), *Concrete construction engineering handbook*. CRC Press.
- Lu, W. Y., Lin, I. J., Hwang, S. J., & Lin, Y. H. (2003). Shear strength of high-strength concrete dapped-end beams. *Journal of the Chinese Institute of Engineers*, *26*, 671–680.
- Mattock, A. H. (2012). Strut-and-tie models of dapped-end beams. *Concrete International*, *34*(2), 35–40.
- Mattock, A. H., & Chan, T. C. (1979). Design and behavior of dapped-end beams. *PCI Journal*, *24*, 28–45.
- Mattock, A. H., & Theryo, T. S. (1986). Strength of precast prestressed concrete members with dapped ends. *PCI Journal*, *31*(5), 58–75.
- Mohamed, R., & Elliott, K. (2008). Shear strength of short recess precast dapped end beams made of steel fibre self-compacting concrete. In *33rd Conference on Our World in Concrete & Structures*, Singapore Concrete Institute.
- Mohammed, S. D., & Mahmoud, T. K. (2015). Strength enhancement of pre-stressed concrete dapped-end girders. *Journal of Engineering*, *21*, 1–16.
- Moreno-Martínez, J. Y., & Meli, R. (2014). Experimental study on the structural behavior of concrete dapped-end beams. *Engineering Structures*, *75*, 152–163.
- Nagrodzka-Godycka, K., & Piotrkowski, P. (2012). Experimental study of dapped-end beams subjected to inclined load. *ACI Structural Journal*, *109*(1), 11–20.
- Nagy-György, T., Sas, G., Dăescu, A., Barros, J. A., & Stoian, V. (2012). Experimental and numerical assessment of the effectiveness of FRP-based strengthening configurations for dapped-end RC beams. *Engineering Structures*, *44*, 291–303.
- P. D. Handbook. (2010). *Precast. Prestressed Concrete Institute*, 2010.
- Peng, T. (2009). *Influence of deta of dapped*. Montreal: McGill University Montréal.
- S.-C. C. E. P. Group. (2005). *The European guidelines for self-compacting concrete: Specification, production and use*. Brussels: International Bureau for Precast Concrete (BIBM).
- Schlaich, J., & Schafer, K. (1991). Design and detailing of structural concrete using strut-and-tie models. *Structural Engineer*, *69*, 113–125.
- Taher, S.-D. (2005). Strengthening of critically designed girders with dapped ends. *Proceedings of the Institution of Civil Engineers-Structures and Buildings*, *158*, 141–152.
- Wang, Q., Guo, Z., & Hoogenboom, P. C. (2005). Experimental investigation on the shear capacity of RC dapped end beams and design recommendations. *Structural Engineering and Mechanics*, *21*, 221.

Publisher's Note

Springer Nature remains neutral with regard to jurisdictional claims in published maps and institutional affiliations.